# CORROSION INHIBITION OF ALUMINIUM ALLOYS BY LAYERED DOUBLE HYDROXIDES: THE ROLE OF COPPER

M. A. TRAVASSOS, C. M. RANGEL

[1] *Instituto Nacional de Energia e Geologia, Fuel Cells and Hydrogen Unit*
*Paço do Lumiar, 22 1649-038*
*Lisboa Portugal*
*antonia.travassos@lneg.pt; carmen.rangel@lneg.pt*

## Abstract

Layered double hydroxides represented by the general formula $[M_2^{2+}M^{3+}(OH)_6]^+X_{1/n}^{n-}.zH_2O$ are being researched as anion-exchange materials with interesting intercalation chemistry that accommodate a wide range of applications, including corrosion resistance.

In this work, it is shown that the formation of layered double hydroxides (LDHs) on the surface of copper-rich Al alloys promotes corrosion resistance. For that purpose a LDH of the type $[M^+M^{3+}{}_2(OH)_6[A^{n-}{}_{1/n}].zH_2O]$, where the intercalated cation is mono-valent Lithium is studied. In Aluminium 2024-T3 or Al-Li 8090, corrosion inhibition was achieved as a result of the formation of a LDH film: $Al_2Li(OH)_7.2H_2O$ or $Al_2Li(OH)_62CO_3.zH_2O$ according to the precursor solution used. LDH´s covered the entire surface of the mentioned alloys, mitigating the galvanic action between the matrix and Cu rich phases, usually responsible for corrosion of the localized type. Inhibition is demonstrated to be under diffusion control. Layered double hydroxides were characterised using X-ray diffraction, FTIR and SEM. The role of copper is examined using an approach that includes a study on pure copper samples.

***Keywords:*** *layered double hydroxides, Cu- rich Al Alloys, corrosion inhibition*

## 1. Introduction

Layered double hydroxides have received considerable attention due to a particular number of attractive properties promoting widespread applications in catalysts, adsorbents, bioactive agents and thin films as protective corrosion coatings [1-4].

Layered double hydroxides (LDH) are lamellar compounds with positively charged layers, constituted by two metallic cations and an intercalated exchangeable hydrated gallery of anions that maintains the system electroneutrality [5]. Most of the layered double hydroxides may be expressed by the general formula $[M^{2+}{}_{(1-x)}M^{3+}I_x(OH)_2[A^{n-}{}_{x/n}].zH_2O$ or $[M^+M^{3+}{}_2(OH)_6[A^{n-}{}_{1/n}].zH_2O]$, where $M^+$, $M^{2+}$ and $M^{3+}$ are mono-, di- and tri-valent metal cations and $A^{n-}$ is the exchangeable anion, [1-2].
The several arrangements of metallic cations, $M^{2+}/M^{3+}$, must assure similarity between the ionic radius, coordination number and lattice energy. The metallic cations layers, with similar ionic radius, are coordinated with six oxygen atoms forming $M^{2+}/M^{3+}(OH)_6$ octahedra. These octahedra form two-dimensional layers that stack together by hydrogen bonding between the hydroxyl groups of adjacent layers [5]. The interlayer or interlamellar region contains water molecules. The amount of water is determined by factors such as the nature of the

interlamellar anions, the water vapor pressure and the temperature. The water molecules are connected to both the metal hydroxide layer and the interlayer anions through extensive hydrogen bonding [5], which are continuously breaking and forming.

The LDH structure supports anion diffusion and the formation of new layered double hydroxides by anionic exchange [6]. The selectivity of anions exchange can be influenced by temperature, the shape and charge density of the guest host layer and the solvent of the intercalation reaction.

In this work, the ability to inhibit localized corrosion of copper-rich Al alloys was assessed when building layered double hydroxides films on the metal surfaces. The study was focused on Al 2024-T3 and Al-Li 8090 alloys, susceptible pitting corrosion and to intergranular, respectively. The corrosion inhibition occurred in both alloys with the in-situ formation of a LDH, in the presence of lithium as intercalation cation, was favoured in a host network of aluminum hydroxide.

## 2. Experimental

Al-Li 8090, 2024-T3 alloys and pure copper from Good Fellow Metals were used as working electrodes. Elemental chemical composition is reported in table1.

*Table 1. Elemental chemical composition (wt%) of Al-Li 8090, Al 2024-T3 alloys and copper used in this work, as working electrodes.*

| Al-alloy | Li wt% | Cu wt% | Mg wt% | Zr wt% | Fe wt% | Si wt% | Mn wt% | Al |
|---|---|---|---|---|---|---|---|---|
| Al-Li 8090 | 2.36 | 1.16 | 0.80 | 0.12 | 0.06 | 0.05 | - | balance |
| Al 2024-T3 | - | 4.50 | 2.00 | - | 0.60 | 0.80 | 0.80 | balance |
| Cu | | 99.999 | | | | | | |

Samples, with an area of ~1cm$^2$, were welded to a conductor wire and embedded in epoxy resin. After mechanical polishing with abrasive SiC paper up to 1200 grit, the samples were washed with distilled water, degreased with ethanol and dried with cool air. Afterwards, aluminum alloy samples were submitted to a surface pre-treatment with NaOH (0.3 wt%) followed by immersion in a $HNO_3$ solution (50 wt%).

The electrochemical measurements were carried out at room temperature in normally aerated solutions. Working solutions were prepared with distilled water and Analar reagents (0.05M $Na_2CO_3$, 0.05M $Li_2CO_3$, 0.1M LiOH and 0.1M NaCl).
An electrochemical cell with a three electrode configuration was used. A saturated calomel electrode (SCE) and a large area platinum wire were used as reference and counter electrodes respectively. Polarization curves were run with a PARC Potentiostat, model 173. The studied

potentials were within the range from -2.0V to +2.0V (SCE). The scan rate, v, was varied from 5 to 200 $mVs^{-1}$ and all potentials are referred to (SCE).

Lamellar double hydroxide compounds were electrochemically formed on Al alloy surfaces and by chemical co-precipitation, for an ex-situ study, from hydroxides and metallic salts in a aqueous solution mixing γ-$Al(OH)_3$ 0.05M and $Li_2CO_3$ 0.05M or Li(OH) 0.1 M, at room temperature. For the latter case experiments were conducted under agitation during 16 hours. The obtained products were dried at 60ºC during 24 hours, before analysis.
Analysis was carried out using a SEM (Scanning Electron Microscope from Philips, Model XL 30 FEG), coupled to EDS. Materials were also characterized by X-Ray Diffraction, XRD, (Rigaku, Geiger-Flex D/Max IIIC) and Fourier Transform Infrared Spectroscopy, FTIR, (Nicolet, model Magna 560).

## 3. Results and Discussion

### *3.1 Layered Double Hydroxides Formation*

In the first part of this work, layered double hydroxides of aluminium and lithium were obtained ex-situ, by chemical co-precipitation, at room temperature from a mixture of γ-$Al(OH)_3$/$Li_2CO_3$ with a molar ratio of 1:1 solutions, according to details given in section 2.

The compound was caracterized by X-Ray Diffraction, SEM and FTIR. The XRD spectrum of the obtained layered double hydroxides is shown in figure 1, with the identification of lithium aluminium hydroxide hydrate ($[Al_2Li(OH)_6]^+OH^-.2H_2O$) and lithium aluminium carbonate hydroxide hydrate ($[Al_2Li(OH)_6]^+{}_2CO_3^{2-}.zH_2O$). The presence of gibbsite γ-($Al(OH)_3$) and zabuyelite ($Li_2CO_3$) is also indicated. Li is coordinated in octahedral positions left empty by $Al^{+3}$. The compounds have a lamellar morphology, as evident in figure1. Lamellae showed an average thickness of 55 nm.

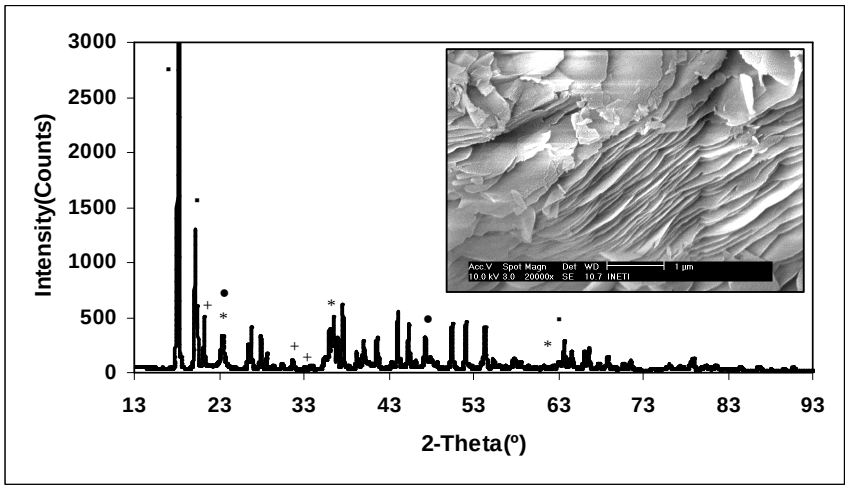


*Fig.1 XRD spectrum and SEM image of lithium aluminium hydroxide formed ex-situ by co-precipitation. ▪Gibbsite γ-$Al(OH)_3$;*Lithium Aluminium Carbonate Hydroxide Hydrate; ●Lithium Aluminium Hydroxide Hydrate; $^+$ Zabuyelite $Li_2CO_3$.*

The treatment of gibbsite [γ-$Al(OH)_3$] with lithium carbonate in aqueous solution promoted the formation of LDH with Li cation and anions intercalation in the guest structure. Crystal structure of the compounds is presented in figure 3.

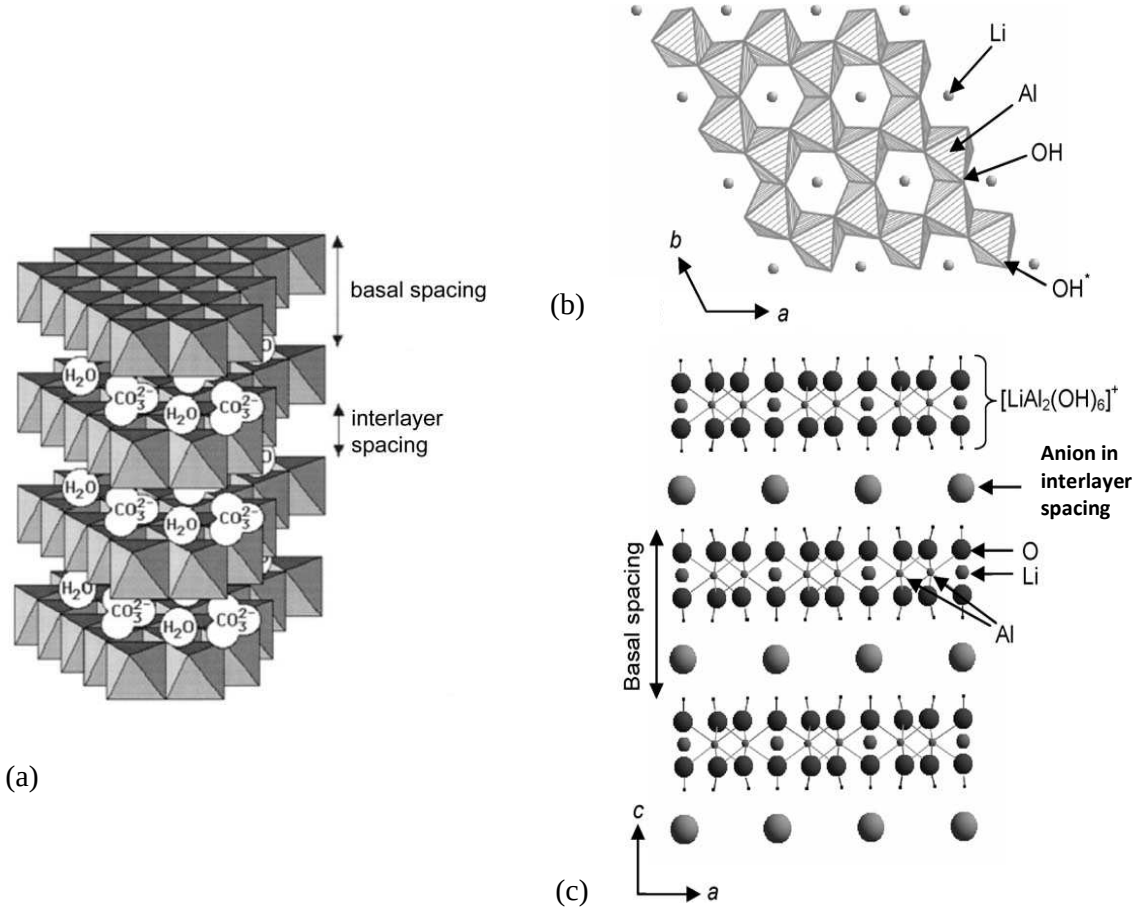


*Fig. 2 Idealized structure of LDH showing carbonate and water in the interlayer spacing (a); crystal structure of lithium intercalated gibbsite projected along the c (b) and b axes (c), respectively* [6,7].

The FTIR spectrum of LDH formed using γ-$Al(OH)_3$ and $Li_2CO_3$ reveals the presence of absorption bands at 3621-3387$cm^{-1}$; 1021$cm^{-1}$; and a doublet at 799-742$cm^{-1}$, associated to O-H vibrations. The absorption bands located at 1495$cm^{-1}$, 1430 $cm^{-1}$ and 862$cm^{-1}$, were correlated to C-O vibrations from the carbonate group, see figure 3. Assymetric stretching mode of free carbonate is normally observed at 1415 $cm^{-1}$[8].

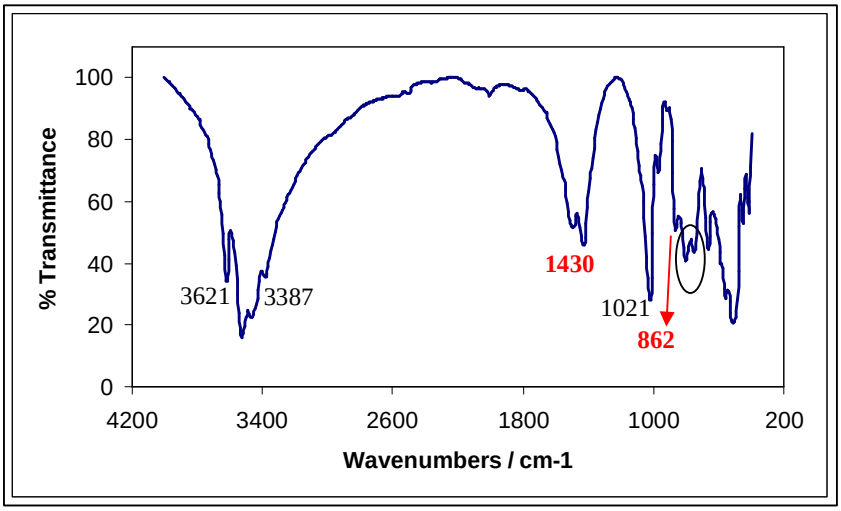


*Fig.3 FTIR spectrum for the compound obtained ex-situ from aluminium hydroxide and lithium carbonate. C-O stretching absorption are shown in red.*

3.2 *Layered Double Hydroxides Formation on Al-alloys surface*

Layered double hydroxides were also obtained by *in situ* formation on aluminium copper-rich alloys by immersion in alkaline solutions of lithium ions (lithium carbonate or lithium hydroxide). In this case the compound formed is represented by the formula $[LiAl_2(OH)_6]X._zH_2O$ or ($LiAl_2$-X), with X representing the exchange anion.

In the case of aluminium alloys 2024-T3, widely used in aerospace and others industrial applications, mechanical properties are conferred by the presence of second phase particles. As it is well known, the presence of the resulting heterogeneous microstructure promotes susceptibility to pitting corrosion. Pitting corrosion is associated to the presence of intermetallic particles such as $Al_2CuMg$, S phase, which denotes an anodic character. Corrosion is found to initiate around the S phase, causing severe pitting of the alloy when exposed to a chloride-containing environment, as observed in figure 4.

The electrochemical behaviour of the Al 2024-T3 alloy after surface pre-treatment was evaluated in a LiOH 0.1M alkaline solution and compared with that obtained without treatment in a near neutral solution of NaCl 0.1M. Polarization curves were run at room temperature in a normally aerated solution and with a scan rate (v) of 12.5 $mVs^{-1}$. Data are shown in figure 5. A shift in the breakdown potential of about 1.5V, between the pitting potential in chloride containing solution ($E_p$= -0.4V) and a breakdown potential of 1.1V observed in lithium containing environment, figure 5b). The film formation is exhibited by SEM image, figure 5(b). The corrosion inhibition occurred by LDH´s formation - $Al_2Li(OH)_7.2H_2O$ e $Al_2Li(OH)_62CO_3.zH_2O$ -, which covered the alloy surface and mitigated the galvanic effect between the alloy matrix and the Cu-rich phases.
The pitting resulted from the selective dissolution of Mg and Al, from the phase S. As dealloying continued, the S phase remnants became Cu-rich, turning into a cathode in relation to the adjacent Al matrix, causing dissolution of the surrounding Al matrix along the S phase.

The EDS spectra in figure 4a) allow qualitatively comparison between the matrix elements, B, and the elements of remnant S phase, $Al_2CuMg$, A. Small metallic particles Cu particles are found to be spread on the matrix inducing the formation of small pits.

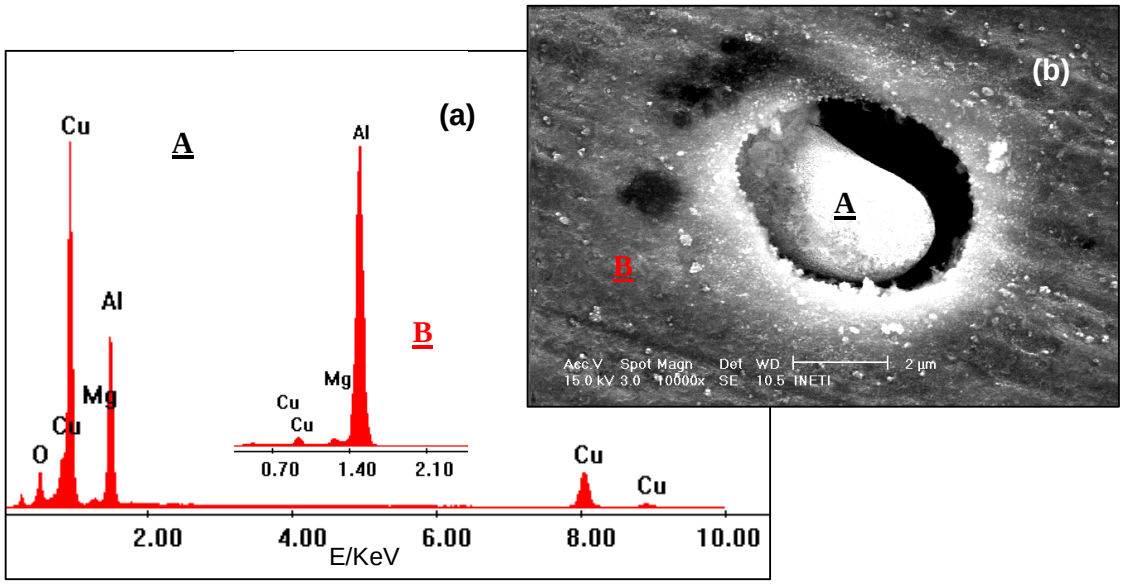


*Fig.4 EDS spectrum for Al2024–T3 alloy (attacked intermetallic (A) and matrix (B), after polarization curves in 0.1M NaCl solution (a); corresponding SEM image (b).*

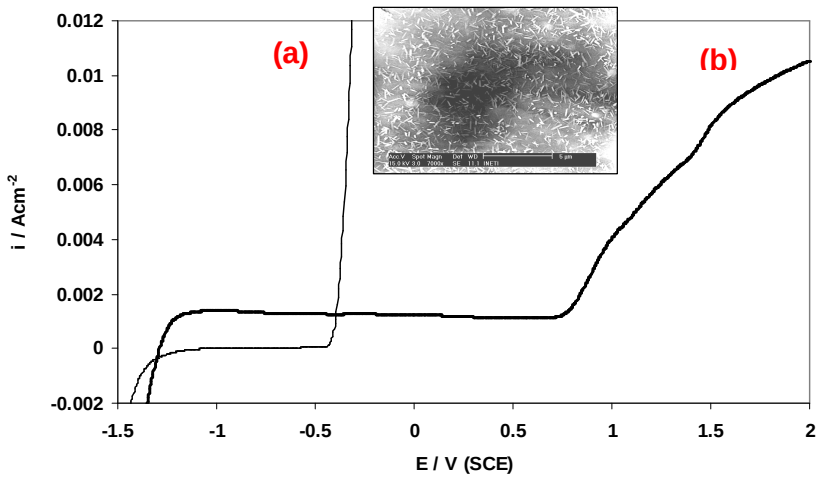


*Fig.5 Polarization curves to Al2024–T3 at scan sweep rate, v, of 12.5mVs$^{-1}$, showing the extension before breakdown when the sample was submitted to treatment in 0.1 M LiOH solution compared to curve in 0.1 M NaCl in the absence of Li ions(a); SEM image related with polarization curve in Li containing environment (b). SEM picture of Al 2024–T3 alloy surface, after polarization.*

In order to study further the inhibition by layered double hydroxide in copper-rich alloys, the electrochemical behaviour of Al-Li 8090 alloy was re-assessed. The alloy is suitable for aeronautical purposes due to their good mechanical properties and low density, but is also known by its susceptibility to localized corrosion.

Polarization curves run at scan rates between 5 and 200 $mVs^{-1}$, for the Al-Li 8090 alloy in alkaline carbonate solutions, are shown in figure 6a). The presence of peak (I) was associated to Al hydroxide formation. This peak is located in the potential ranges between -1.3 e -1.1V, depending on potential scan rate.
A second peak (II) was localized at ~-0.200V (SCE), and was related with Cu oxidation/dissolution process, which were evidently inhibited in presence of lithium, see figure 6b). A third peak is detected at potentials higher than 1V due to formation of Cu (III) species [9-11]. This process is also inhibited when in presence of lithium ions in solution.
The SEM images point towards the existence of intergranular corrosion on the Al-Li 8090 alloy surface after exposition in sodium carbonate solution, figure 6(a), with selective dissolution of T phases $T_1(Al_2CuLi)$ or $T_2(Al_6CuLi_3)$, anodic phases located in the grain and subgrain boundaries respectively.

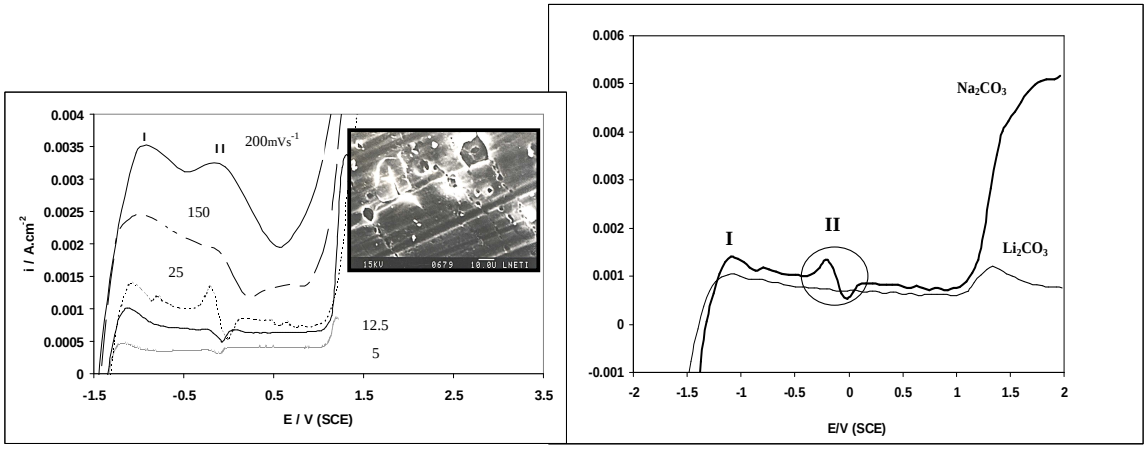


*(a)* *(b)*

*Fig.6 Polarization curves at several sweep scan rates, from 5 up to 200 $mVs^{-1}$ for Al-Li 8090 alloy in 0.05 M $Na_2CO_3$ solution and SEM picture denoting intergranular corrosion in Al-Li 8090 alloy (a); Comparison of polarization behavior in 0.05 M $Na_2CO_3$ and in 0.1M $Li_2CO_3$ solutions at a scan rate of 25$mVs^{-1}$(b).*

After analysis of the electrochemical behaviour as a function of the scan rate, peak (I) is associated to a process controlled by diffusion in solution, in agreement with a linear dependence with a slope value of 0.45, in the log-log plane, of the current density with the scan rate. [12-14].
Analogous analysis of the effect of scan rate, in the case of lithium ions containing solution, gave place to two different slopes with a value of 0.67, at high scan rates, and a value of 0.27, at low sweep scan rates. In the first case a process of aluminium diffusion in solution was associated, while in the second case a process in solid state [15] is thought to be related with intercalation Li ions and formation of the layered double hydroxide. The formation of the double hydroxide inhibits the processes related to copper dissolution as evident in figure 6b).
A SEM picture of the surface of Al-Li 8090 alloy is shown in figure 7.

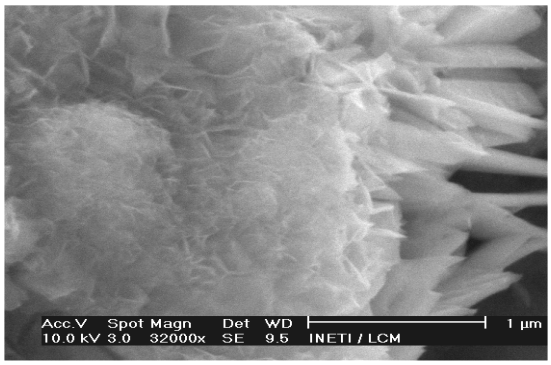


Fig.7 SEM images for the surface of Al-Li 8090 alloy after polarization in the presence of of Li ions in solution

In view of the inhibition of copper related redox processes, demonstrated during polarization in the presence of lithium ions, a study using pure copper was undertaking in the same experimental conditions as for the Al alloy.

The electrochemical behaviour of copper in alkaline solutions is rather complex. In this work it is analyzed using sectioned voltammograms in order to visualize more clearly the corresponding anodic/cathodic processes at relevant potential windows. Figure 8a) shows sectioned voltammograms for copper (steps 0.25 V) in an alkaline solution of sodium carbonate, exhibiting typical copper oxidation / reduction peaks, corresponding to Cu(I) and Cu(II) species. Also noticeable is the development of an ohmic like-resistance – linear variation of the potential with the current density at anodic potentials (evident for E> -0.02V), this is thought to be responsible for the continuous displacements (towards more cathodic potentials) of both of the cathodic peaks as a result of the formation of a salt film on the copper surface. The salt film increases in thickness with increasing polarization, making reduction of copper species increasingly difficult and thus justifying the displacement of the reduction peaks.

In the presence of lithium ions, the main characteristics of the voltammograms are associated to lower current densities at anodic potentials, when compared to the behaviour in solutions in the absence of lithium, see figure 8b).
The SEM observation shows a porous film covering the surface with a structure in the form of intersecting needle like precipitate, figure 8b). A layer of CuO is formed leading to surface extensive coverage. CuO film does not seem to thicken much with potential. This is probably due to the solubility of cupric ions at the pH (~11) used in this work, being probable that constant thickness is achieved by a steady-state film-growth dissolution process.

The electrochemical evidence showed in this work also points towards the formation of a base layer of $Cu_2O$, see equation (1), indicated by the potential window in which the peaks are revealed. A porous structure of the layer is suggested by the relative charge of cathodic peak Ic compared to the charge of the corresponding anodic peak in figure 8b). Metal dissolution as $Cu^{2+}$ species occurs. The oxidative dissolution renders copper hydroxides, see equation (2) that leads to the formation of CuO at appropriate potentials as indicated in the figure, both by the anodic shoulder and by the appearance of its corresponding cathodic peak Ic, equation 3. Oxidative dissolution of $Cu_2O$ may also occur according to equation (4).

$$Cu + 2OH^- \rightarrow Cu_2O + H_2O + 2e \quad (1)$$

$$Cu + nOH^- \rightarrow Cu(OH)_n^{2-n} + 2e \quad (2)$$

$$Cu(OH)_n^{2-n} \rightarrow CuO + (n-2)OH^- + H_2O \quad (3)$$

$$Cu_2O + H_2O + (2n-2)OH \rightarrow Cu(OH)_n^{2-n} + 2\,e \quad (4)$$

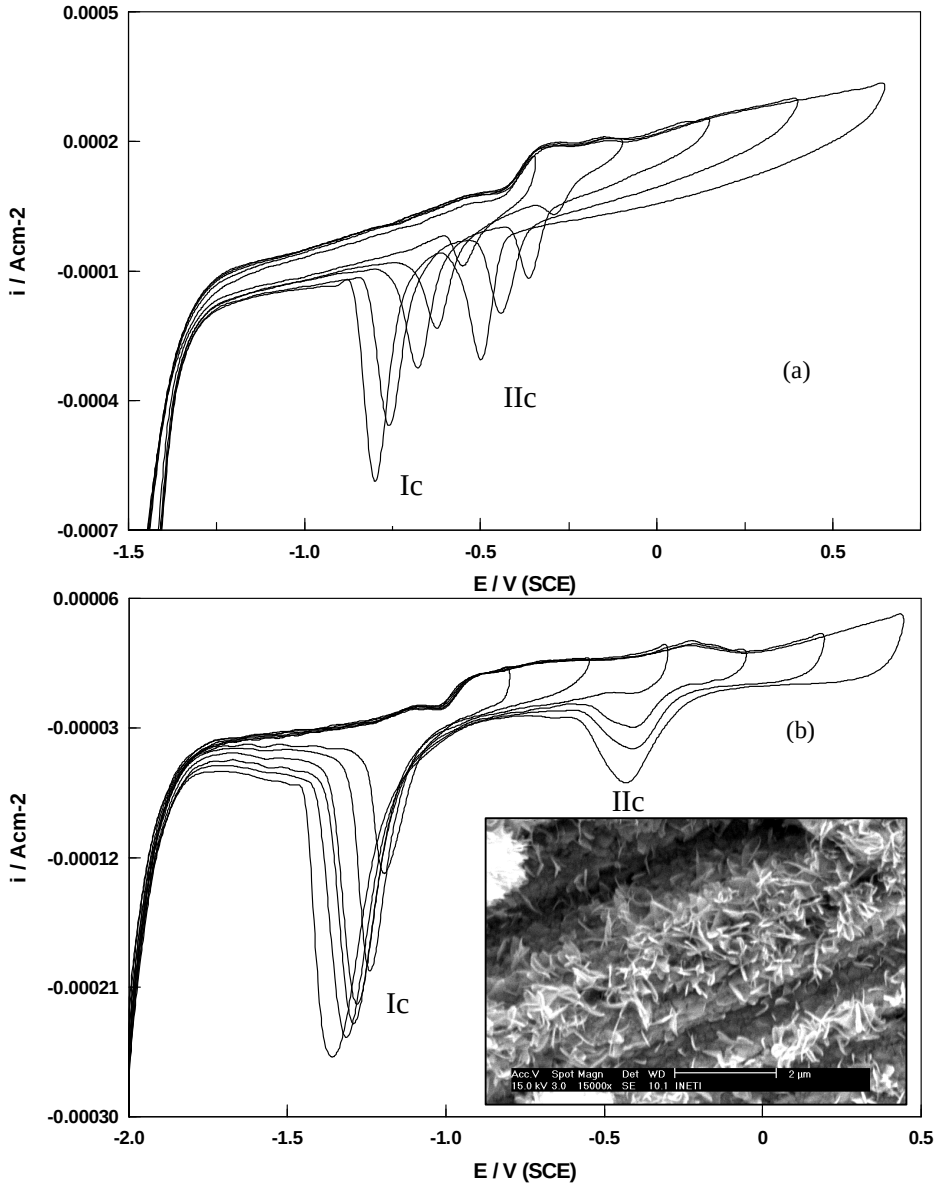


*Fig. 8 Sectioned cyclic voltammograms for Cu in 0.1M LiOH and 0.05M $Na_2CO_3$ solutions at room temperature, in normally aerated conditions and at a sweep scan rate, v, of 12.5 $mVs^{-1}$. SEM image related with film formation after cyclic voltammogram of Cu in 0.1M LiOH.*

## 4. Conclusions

- Localized corrosion inhibition in structural Cu-rich aluminium alloy was possible as a result of layered double hydroxides formation, constituted by $Al_2Li(OH)_7.2H_2O$ and $Al_2Li(OH)_62CO_3.zH_2O$, that covered the alloy surface reducing the galvanic action between the alloy matrix and the copper-rich phases.
- In the Al 2024-T3 alloys the process was associated to the corrosion inhibition of phase S, while in the Al-Li 8090 alloy to T phases localized at grain and sub-grain boundaries.
- Evidenced is produced, by cyclic voltammetry of Al alloys and pure copper, of the involvement of copper in the inhibition of localised corrosion.
- Inhibition related processes are under diffusion control.

## 5. References


[1] –Li, Lei, Mo Dan, Chen, Da-Zhou, Chinese J. Chem., **23** (2005) 266.
[2] – G.R. Williams, D. O'Hare, J. Mater. Chem., **16** (2006) 3065.
[3] – G.R. Williams, D. O'Hare, J. Phys. Chem. B, **110** (2006) 10619.
[4] – O. Saber, H. Tgaya, Rev. Adv. Mater. Sci., **10** (2005) 59.
[5] – A.I. Khan, D. O'Hare, J. Mater. Chem., **12** (2002) 3191.
[6] –Shan-Li Wang, Chia-Ya Cheng, Yu-Min Tzou; Ren-Bao Liaw, Ta-Wei Chang, Jen-Hshuan Chen, J. Hazardous Materials, **147** ( 2007) 205.
[7] –D.G. Evans and X.Duan, Chem. Commun., **5** (2006) 485.
[8] –S.J.Palmer, R.L.Frost, T.Ngugen, Coordination Chemistry Reviews, **253** (2009) 250-267.
[9] – G. Kear, B.D. Barker, F.C. Walsh, Corros. Sci., **46** (2004) 109.
[10] – P. Traverso, A. M.Beccari, G. Poggi, Br. Corros. J., **30** (1995) 227.
[11] Y. Sepulveda, C.M. Rangel, R.A. Silva, M.A. Páez, P. Skeldon, G.E. Thompson, ATB Metallurgie, **43** (2003) 407.
[12] – C.M. Rangel, M.A. Travassos, Corros. Sci., **33** (1992) 327.
[13] – C.M.Rangel, M.A. Travassos, Surf. and Coat. Techn., **200** (2006) 5823.
[14] – M.A. Travassos, C.M. Rangel, EUROCORR2005, paper 543, Lisboa, Portugal, 2005.
[15] – C.M. Rangel, R. A Leitão, I.T.E. Fonseca, Electrochim. Acta, **34** (1989) 255.